Preparation and evaluation system for NEA GaN photocathode

XIAOHUI WANG*, BENKANG CHANG, YUNSHENG QIAN, YUJIE DU, HONGGANG WANG, BIAO LI
Department of Electronic Engineering and Optoelectronic Technology, Nanjing University of Science and Technology, Nanjing, Jiangsu 210094, People's Republic of China

To obtain and evaluate negative electron affinity (NEA) GaN photocathode, preparation and evaluation system has been designed. The system includes multi-information test system, ultrahigh vacuum (UHV) activation system, and surface analysis system. GaN photocathode, which had been etched by a 2:2:1 solution of sulfuric acid, hydrogen peroxide and de-ionized water, was analyzed by the surface analysis system. Then the GaN photocathode was transferred to the UHV system where it was cleaned by heating at 710 , and soon was activated by Cs/O. By use of the multi-information test system, vacuum level and composition of the residual gas were recorded during the heating process, photocurrent was recorded during the activation, and quantum efficiency of NEA GaN photocathode was tested.

(Received July 20, 2011; accepted September 15, 2011)

Keywords: Negative electron affinity, GaN photocathode, Preparation and evaluation system

1. Introduction

Gallium nitride (GaN) is a new kind of semiconductor material, which has excellent properties of low dielectric constant, corrosion resistance, high temperature resistance, and radiation resistance. GaN has many applications in high power, temperature electronics, and high radiation environment [1-7]. Negative electron affinity (NEA) GaN photocathode has superior performing of high quantum efficiency (QE), because its bottom of conduction band is lower than the vacuum level. NEA GaN photocathode also has character of low dark current, and concentrative emitting electron energy distribution [8-14]. The band gap of GaN reaches 3.4 eV at room temperature, so it is a natural "solar blind" material. Therefore, NEA GaN photocathode can be extensively applied in lithographic manufacture, ultraviolet detection, atmospheric monitoring, fire alarm technology, and other fields [15-23].

NEA GaN photocathode can be obtained by Cs/O activated in vacuum environment. In the preparation, many factors will influence the performance of NEA GaN photocathode finally, including the chemical cleaning and heating temperature, the quantity of Cs/O, and the vacuum level of environment. So a good and convenient preparation system becomes necessary and important.

In this text, we desired the NEA GaN photocathode preparation and evaluation system based on the NEA GaAs photocathode system. GaN samples were activated, the information during preparation was recorded, and after activation QE of the NEA GaN photocathode was tested.

2. Experimental system

The NEA GaN photocathode preparation and evaluation system is consisted of the multi-information test system, ultrahigh vacuum (UHV) activation system, and surface analysis system, as shown is Fig. 1.

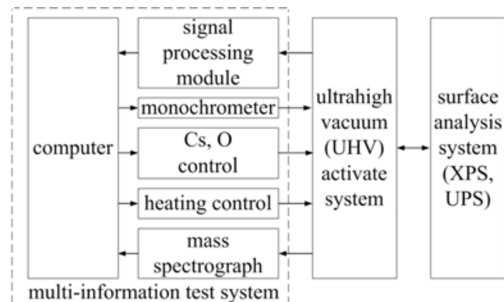

Fig. 1. NEA GaN photocathode preparation and evaluation system.

The multi-information test system can control the activation light, the Cs/O quantity, and the heating temperature. Photocurrent can be picked up by signal processing module during and after activation. The accuracy of measurement is 1 nA. The spectrum measuring range is from 240 to 400 nm. A quadrupole mass spectrograph (QMS) is used to test the composition of the residual gas in UHV system.

The UHV system includes mechanical pump, turbo molecular pump, ionization pump, and vacuum chamber. The pressure of the vacuum chamber can reach 3.3×10^{-8} Pa at best. As Fig. 2 shown, the vacuum chamber is connected to QMS, vacuum gauge, heating facility, vacuum pump, and the surface analysis system by flange. There are quartz windows for observation, and light is illuminated through quartz window too, including both reflection-mode (*r*-mode) and transmission-mode (*t*-mode).

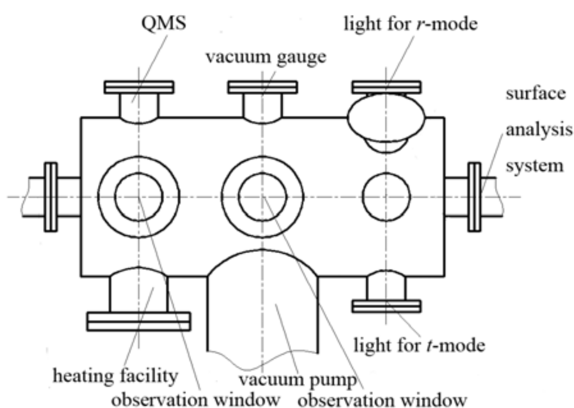

Fig. 2. The UHV vacuum chamber.

The surface analysis system is consisted by a Perlin Elmer 5300 series X-ray photoelectron spectrometer (XPS) and ultraviolet photoelectron spectrometer (UPS). The XPS has two targets of Mg and Al to meet different needs. The glancing angle of the XPS is from 0 to 90 °, and the measuring range is from 1400 to 0 eV.

3. Experiment and results

The experiment samples are GaN films, which are grown by metal-organic chemical vapor deposition (MOCVD) on *c*-plane sapphire (Al_2O_3) substrates with a $Ga_{1-x}Al_xN$ buffer layer. The GaN layer is p-type doped with the concentration of 10^{17} cm^{-3}.

GaN was etched by a 2:2:1 solution of sulfuric acid, hydrogen peroxide and de-ionized water firstly, and then was put in the surface analysis system. XPS electron spectroscopy of GaN (0001) after chemical cleaning is shown in Fig. 3. From Fig. 3 it can be seen, after chemical cleaning, Ga3d, N1s, C1s, and O1s are detected, which indicates that contaminations on GaN (0001) are C and O mainly.

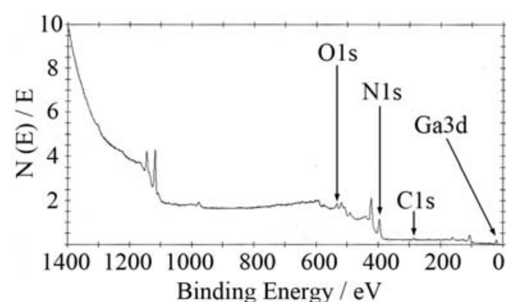

Fig. 3. XPS electron spectroscopy of GaN (0001) after chemical cleaning.

GaN was transferred to the UHV system where it was cleaned by heating at 710 for 25 min. During the heating process, vacuum level of the UHV system and composition of the residual gas were recorded, which is shown in Fig. 4 and Fig. 5. In Fig. 4, curve 1 is the temperature, and curve 2 is the vacuum level. The vacuum level falls with increase of temperature, and the vacuum level reaches lowest at 710 ℃. As cooling the vacuum level resumed to the initial level.

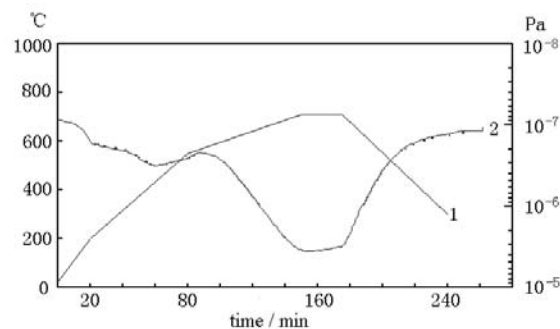

Fig. 4. Temperature and vacuum curve during the heating of GaN photocathode.

In UHV system, composition of the residual gas at 710 ℃ was recorded by the QMS. As Fig. 5 shown, the dominant residual gas in the chamber is in the region around 2, 18, 28 and 44, corresponding to H_2, H_2O, CO or N_2, and CO_2.

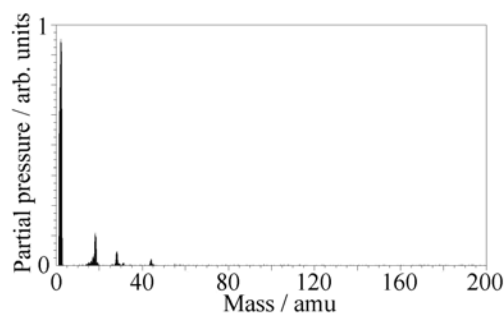

Fig. 5. Mass spectrum of the residual gas.

After the cleaning process, GaN photocathode was activated by Cs/O, and the quantity of Cs and O is controlled accurately by the multi-information test system. The photocurrent during the activation is shown in Fig. 6. From Fig. 6, it can be seen that Cs was performed with GaN at room temperature (20 ℃) until a maximum photocurrent was obtained. Under a constant Cs flux, the oxygen was not admitted into the chamber until the photocurrent stopped increasing. When the photocurrent reached a peak, the oxygen current was cutoff, and the photocurrent dropped. After the oxygen switch was turned on and off several times, the photocurrent reached its maximum level.

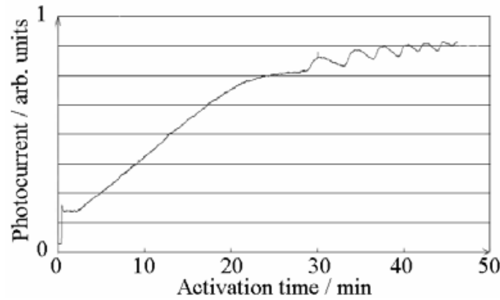

Fig.6. Photocurrent during the Cs/O activation.

The *r*-mode and *t*-mode QE of NEA GaN photocathode between 3.1 and 5.2 eV is shown in Fig. 7, which corresponding 240 – 400 nm. Curve 1 is the *r*-mode QE, and curve 2 is the *t*-mode. It can be seen from the figure that the *r*-mode QE is high and flat between 240 and 350 nm, and the maximum QE reach 30% at 240 nm. For the *t*-mode, there is high and flat quantum yield between 255 and 355 nm, and the maximum QE reaches 13% at 290 nm. When the wavelength of the incident light extends to 355 nm, the QE of both modes begin to drop rapidly with increase of the wavelength, and a distinct inflection point is formed at 355 nm. The QE falls to 3.5% at the threshold wavelength of 365 nm, and there is only 0.1% QE at the 385 nm, which demonstrates the excellent long-wave cut-off property.

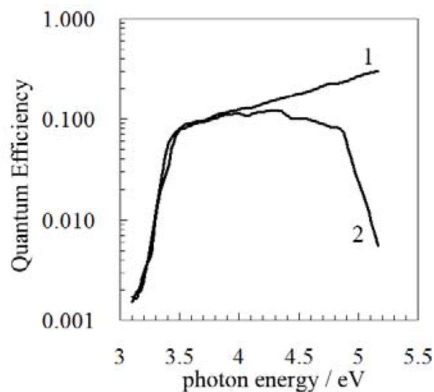

Fig. 7. The r-mode and t-mode QE of NEA GaN photocathode.

QE of the *t*-mode GaN photocathode decreases at short wavelength less than 250 nm, which is different from the *r*-mode, as shown in Fig. 7. QE of the *t*-mode reduces to about 0.6% at 240 nm while there is still a high quantum yield for the *r*-mode. This is because the incident light is shone on the sapphire substrates in the *t*-mode, and the light must go through the substrate and the $Ga_{1-x}Al_xN$ buffer layer before reaching the GaN emission layer. The $Ga_{1-x}Al_xN$ buffer layer has a larger band gap than the GaN, and it has a higher absorption coefficient for the short wavelength light. Most of the short wave will be absorbed in the buffer layer and is difficult to reach the GaN emission layer, so the QE of the *t*-mode NEA GaN photocathode will go down eventually in the short wavelength.

4. Conclusion

In conclusion, we desired the NEA GaN photocathode preparation and evaluation system. GaN samples were activated, and after activation QE of the NEA GaN photocathode was tested. The maximum QE *r*-mode reach 30% at 240 nm, and *t*-mode reaches 13% at 290 nm.

Acknowledgements

Project supported by the National Natural Science Foundation of China (Grant No. 60871012), and Project supported by the National Key Laboratory of Science and Technology Foundation on Low Light Level Night Vision (Grant No. J20110104).

References

[1] E. P. Samuel, D. S. Patil. Optoelectron. Adv. Mater. **1**, 394 (2007).
[2] I. V. Bazarow, B. M. Dunham, X. Liu, M. Virgo, A. M. Dabiran, F. Hannon, H. Sayed, J. Appl. Phys. **105**, 083715 (2009).
[3] O. H. W. Siegmund, J. S. Hull, A. S. Tremsin, J. B. McPhate, A. M. Dabiran, Proc. SPIE **7732**, 77324T (2010).
[4] O. H. W. Siegmund, A. S. Tremsin, J. V. Vallerga, J. B. McPhate, J. S. Hull, J. Malloy, A. M. Dabiran, Proc. SPIE **7021**, 70211B (2008).
[5] O. H. W. Siegmund, J. V. Vallerga, J. B. McPhate, A. S. Tremsin, Proc. SPIE **5488**, 789 (2004).
[6] O. H. W. Siegmund, Nucl. Instr. and Meth. A **525**, 12 (2004).
[7] M. P. Ulmer, Proc. SPIE **6189**, 61890W (2006).
[8] M. P. Ulmer, B. W. Wessels, B. Han, J. Gregie, A. Tremsin, O. H. W. Siegmund, Proc. SPIE **5164**, 144 (2003).
[9] I. Mizuno, T. Nihashi, T. Nagai, M. Niigaki, Y. Shimizu, K. Shimano, K. Katoh, T. Ihara, K. Okano, M. Matsumoto, M. Tachino, Proc. SPIE **6945**, 69451N (2008).
[10] A. A. Pakhnevich, V. V. Bakin, G. É. Shaĭbler, A. S.

Terekhov, Phys. Solid State **49**, 2070 (2007).
[11] J. Stock, G. Hilton, T. Norton, B. Woodgate, S. Aslam, M. Ulmer, S. Aerospace, Proc. SPIE **5898**, 58980F (2005).
[12] F. Machuca, Z. Liu, J. R. Maldonado, S. T. Coyle, P. Pianetta, R. F. W. Pease, J. Vac. Sci. Technol. B **22**, 3565 (2004).
[13] F. Machuca, Y. Sun, Z. Liu, K. Loakeimidi, P. Pianetta, R. F. W. Pease, J. Vac. Sci. Technol. B **18**, 3042 (2000).
[14] O. E. Tereshchenko, G. É. Shaĭbler, A. S. Yaroshevich, S. V. Shevelev, A. S. Terekhov, V. V. Lundin, E. E. Zavarin, A. I. Besyul'kin, Phys. Solid State **46**, 1949 (2004).
[15] Q. Yunsheng, C. Benkang, Q. Jianliang, Z. Yijun, F. Rongguo, Q. Yafeng, Proc. SPIE **7481**, 74810H (2009).
[16] J. Qiao, B. Chang, Y. Qian, X. Du, Y. Zhang, X. Wang, Proc. SPIE **7658**, 76581H (2010).
[17] J. Qiao, B. Chang, Y. Zhi, T. Si, Y. Gao, Proc. SPIE **6621**, 66210K (2008).
[18] S. Fuke, M. Sumiya, T. Nihashi, M. Hagino, M. Matsumoto, Y. Kamo, M. Sato, K. Ohtsuka, Proc. SPIE **6894**, 68941F (2008).
[19] S. Uchiyama, Y. Takagi, M. Niigaki, H. Kan, H. Kondoh, Appl. Phys. Lett. **86**, 103511 (2005).
[20] A. M. Dabiran, A. M. Wowchak, P. P. Chow, O. H. W. Siegmund, J. S. Hull, J. Malloy, A. S. Tremsin, Proc. SPIE **7212**, 721213 (2009).
[21] T. Norton, B. Woodgate, J. Stock, G. Hilton, M. Ulmer, S. Aslam, R. D. Vispute, Proc. SPIE **5164**, 155 (2003).
[22] F. S. Shahedipour, M. P. Ulmer, B. W. Wessels, C. L. Joseph, T. Nihashi, IEEE J. Quan. Elec. **38**, 333 (2002).
[23] X. H. Wang, B. K. Chang, L. Ren, P. Gao, Appl. Phys. Lett. **98**, 082109 (2011).

*Corresponding author: bxezwxh@126.com